Experimental studies on the behaviour of headed shear studs for composite beams in fire

Ohk Kun Lim*[1,2], Sengkwan Choi [2], Sungwook Kang [3], Minjae Kwon [3] and J. Yoon Choi [3]

[1] *R&D Laboratory, Korea Fire Institute, 331 Jisam-ro, Gyeonggi-do, 17088, Republic of Korea*
[2] *School of the Built Environment, Ulster University, Newtownabbey, BT37 0QB, UK*
[3] *Fire Safety Centre, Korea Conformity Laboratories, 73 Yangcheong 3-gil, Cheongju, 28115, Republic of Korea*

Abstract. Steel and concrete composite structures are commonly applied in multi-story buildings as they maximise the material strength through composite action. Despite the popularity of employing a trapezoidal deck slab, limited experimental data are available under elevated temperatures. The behaviour of the headed shear stud embedded in a transverse trapezoidal deck and solid slab was investigated at both ambient and fire conditions. Twelve push-out tests were conducted according to the ISO 834 standard fire utilising a customised electric furnace. A stud shearing failure was observed in the solid slab specimen, whereas the failure mode was changed from a concrete-dominated failure to the stud shearing in the transverse deck specimen with an increase in temperature. Comparisons between the experimental observations and design requirements are presented. The Eurocode design guidance on the transverse deck slab gives a highly conservative estimate for shear resistance. A new design formula was proposed to determine the capacity of the shear connection regardless of the slab type when the stud shearing occurs at high temperatures.

Keywords: composite beam; headed shear stud; push-out test; transverse deck; fire

1. Introduction

Fire safety has become a significant design criterion in modern construction owing to increased building sizes, as well as the existence of various combustible materials in them. Several design guidelines, such as the Eurocode and International Building Code (ICC 2017), recommend that the building should withstand fire without collapsing for a minimum duration for the safety of the occupants and firefighters; the fire resistance rating depends on the building purpose and component type. To meet this design criterion, a load-bearing capacity should be higher than any induced load, including the effect of fire. Composite beams have many advantages, such as high stiffness, long span length and small beam depth, compared to a non-composite design because the material merit is maximised by a composite action. A composite interaction in a beam is achieved by a shear connection between the steel beam and concrete slab. Thus, the shear connector is a crucial element to maintain the stability of the composite beam.

Structural performance of shear connections has been widely investigated using experimental and numerical methods. A headed shear stud embedded in a solid concrete slab was evaluated with various parameters such as stud shank damage, percentage of reinforcement, concrete property and number of studs (Kumar and Chaudhary 2019, Qi et al. 2017, He et al. 2017, Luo et al. 2016, Xu and

Sugiura 2014). As the failure mechanism of the shear connection varies depending on concrete slab types, the behaviour of the shear connection with a profiled steel sheeting was also analysed with respect to a deck configuration, stud location and concrete strength (Sun et al. 2019, Nellinger et al. 2017, Qureshi et al. 2011, Ellobody and Young 2006). Few studies have addressed the effect of temperature on shear connections to predict the structural stability in case of fire (Davoodnabi et al. 2019, Mashiri et al. 2017, Rodrigues, 2014, Wang 2012). Furthermore, limited experiments have been conducted concerning shear studs embedded in a trapezoidal deck slab at elevated temperatures (Shahabi et al. 2016).

The capacity of the headed shear stud at high temperatures was initially investigated by Zhao and Kruppa (1996) using high-temperature push-out tests. The shear resistance was evaluated by placing each specimen on a slot of a furnace to simulate a fire condition. Hot gas rose from the furnace slot to the bottom of the specimen based on the ISO 834 standard fire. A total of 35 push-out tests were carried out by inducing heat and constant load. Most of the specimens used were headed shear studs embedded in a solid slab, and a shearing occurred around the stud root area. A temperature ratio of the stud to steel flange was investigated to express a shear resistance reduction with reference to the flange temperature. The stud temperature was measured at the weld collar, which was defined as 5 mm above the bottom of the stud. The temperature ratio was decreased to around 40% at the beginning of the heating process, and it did not exceed 80% until the flange temperature approached 700°C. Zhao and Kruppa (1996) reported a strength reduction rate with respect to the

---

*Corresponding author, Ph.D. Student,
E-mail: terence@kfi.or.kr

temperature of the shear stud and concrete. These findings were adopted in EC4-1-2 (CEN 2014b) to calculate a shear resistance at high temperatures; the strength reduction rate is multiplied by the shear resistance at ultimate limit state (ULS) depending on the cause of failure.

Twenty-four push-out tests were conducted by Chen et al. (2012) incorporating a headed shear stud in a solid, parallel and transverse deck slab at both ULS and fire limit state (FLS). The load-bearing capacity was investigated by inducing a displacement load when the stud temperature approached a designated value, which was measured 10 mm from the bottom of the shear stud because the temperature rate of increase was different from the ISO 834 standard fire. The stud shearing failure was observed in the solid and parallel deck slab, whereas the failure mode was changed from a concrete rib shearing to the stud shearing at around 500℃ of the stud temperature in the transverse deck specimen. The shear resistance was reduced by 60% and 35% when the shear stud was embedded in the solid and transverse deck slab at the stud temperature of 600℃.

Yasuda et al. (2008) carried out a modified push-out test using a specimen with a one-sided concrete slab. The opposite side was placed on a heating apparatus. Five transverse trapezoidal deck specimens having two studs in a rib with a staggered position were prepared. The specimens subjected to the ISO 834 standard fire condition while a constant load was applied. When the stud temperature reached 685℃, the shear resistance was reduced to 26% of its shear resistance at ULS. They argued that the most critical parameter to determine the shear strength in the fire condition is the temperature at the bottom of the shear stud.

Steel-framed construction has been widely used in the UK, which has been over 65% of the multi-story, non-residential building market for the last two decades (McCam-Bartlett 2019). In composite construction, a trapezoidal deck is commonly utilised because it plays a role as both a platform for stud welding and reinforcement bar arranging as well as a formwork during concrete casting. However, the analytical calculation method of the shear resistance at FLS in the current EC4-1-2 (CEN 2014b) is based on the push-out tests using solid slab specimens. Therefore, it is necessary to investigate the structural capacity of the shear connection at high temperatures when utilising a transverse deck slab.
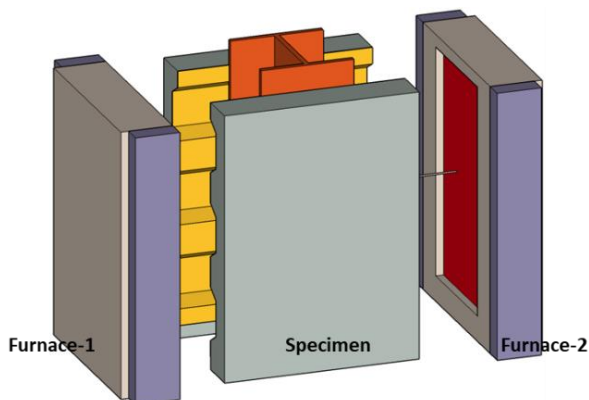
The objective of this study is to determine the influence of temperature on the shear resistance in a composite structure. Failure modes for different slab types were also observed. Twelve push-out tests were carried out under ambient and fire conditions by incorporating customised heating equipment. These results were compared to the design guidance of EC4-1-2 (CEN 2014b) and ANSI360-10 (2010), and a new design criterion is subsequently proposed.

2. Experimental program

2.1 Test setup and specimens

The standardised push-out test in EC4-1-1 (CEN 2009) is specialised for a headed shear stud embedded in a solid slab. There is, however, no guidance for either a trapezoidal deck specimen or a high-temperature experiment. Hicks (2009) proposed a push-out test specimen utilising a trapezoidal deck by enlarging the concrete slab with two levels of shear stud installation. The widened concrete slab helps to avoid cracking at the side section of the concrete ribs in the case of a concrete pull-out failure. The stud arrangement inhibits an artificial failure mode caused by the rotation of the rib. For this reason, the standard push-out test specimen of EC4-1-1 (CEN 2009) was modified to incorporate a transverse deck according to the recommendation of Hicks (2009).

A customised electric furnace was designed according to the configuration of the push-out test specimen. It can replicate the ISO 834 standard fire by applying heat from both sides of the specimen, as depicted in Fig. 1. Two heating panels were attached to the specimen, and the top and bottom sides were insulated to prevent heat loss during the heating process.

The Multideck 60-V2 was used for the trapezoidal deck, which has a height of 61 mm and an average breadth of 155 mm. A 19-mm diameter headed shear stud with a height of 100 mm was welded through the 1.2-mm deck to a steel flange using an automatic welding gun at a favourable side; the distance from the mid-height of the deck in the loading direction to the centre of the shear stud was 117.5 mm. In addition, the shear stud was welded directly to the steel flange when utilising the 0.9-mm deck, which formed a 34-mm diameter hole at the stud location. A 1100-mm long Universal Beam (UB) with dimensions 350×350 and a unit weight of 156 kg/m was used as the steel section. A 10-mm diameter ribbed bar was placed on the deck shoulder for reinforcement. The size of the concrete slab was 750 mm × 1050 mm with a depth of 150 mm. The specific dimensions of the specimen are provided in Fig. 2. A solid slab specimen was also designed to compare the stud behaviour under elevated temperatures; the same steel and concrete sections were used, and the only difference was the absence of the steel sheeting. Table 1 presents the specification of the twelve specimens.

2.2 Materials and instruments

The material properties of the concrete slab and shear

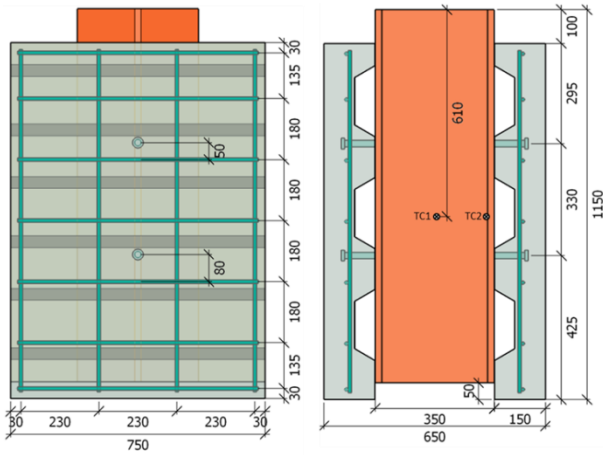Fig. 1 Assembly drawing of the high-temperature test set-up

Fig. 2 Dimensions and thermocouple (TC) locations of the push-out test specimen

stud were evaluated. Cylindrical concrete specimens with a 100-mm diameter and 200-mm height were used to obtain the compressive strength. The mean values of the concrete cylinder compressive strengths f_{cm} were 51 MPa and 32 MPa. The elastic modulus, tensile strength and characteristic compressive strength of concrete were calculated based on EC2-1-1 (CEN 2014a). The shank part of the headed shear stud was machined to make a tensile test coupon in accordance with ISO 6892-1 (ISO 2016). The average yield and ultimate stresses were 415 MPa and 473 MPa with an elongation of 25%.

2.3 Test procedure

The basic concept of the experimental procedure follows EC4-1-1 (CEN 2009) which specifies an initial cyclic loading and measuring range of the applied load. All the specimens experienced a cyclic loading phase with a range of 30% to 5% of an established failure load to break the bonds between the steel flange and concrete slab and

stabilise the specimen; the failure load was calculated by EC4-1-1 (CEN 2009). Then, a displacement load was applied immediately after the cyclic loading at ULS. The load-slip behaviour was measured until the applied load was reduced to 20% of the maximum obtained strength. In the case of the high-temperature experiment, a specimen was subjected to the ISO 834 standard fire condition by applying a constant load which was 20% to 60% of the established failure load. Although the load-slip relationship cannot be collected from this procedure, it is suitable to replicate a fire situation. A fire resistance time and slippage can be achieved through the high-temperature experiment.
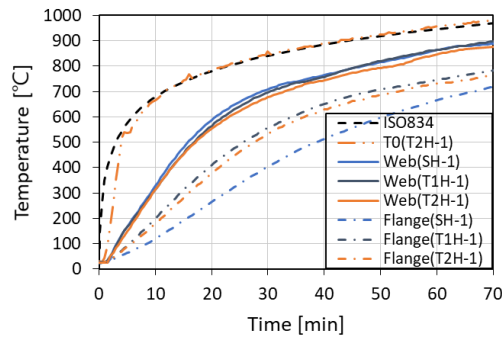
An applied load, relative slip and temperatures were measured during the push-out tests. A square plate swivel jig was placed between the steel beam and actuator which has the maximum capacity of 2500 kN. Three linear variable differential transformers (LVDT) were installed to measure the vertical and lateral displacement at each slab as shown in Fig. 3. A relative slip between the loading plate and concrete slab was obtained using LVDT 1 and LVDT 2.
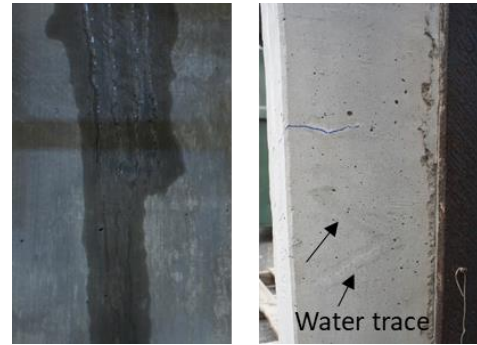

Fig. 3 Furnace and LVDT setup for the high-temperature experiment

Table 1 Detailed descriptions of the test specimens

Specimen	Slab type	Profiled steel sheeting thickness [mm]	Stud welding method	Concrete strength [f_{cm}, MPa]	Test condition
S-1	Solid	-	Direct welding	51	ULS
S-2					
SH-1					FLS
T1-1	Transverse deck	1.2	Through-deck welding	51	ULS
T1-2					
T1H-1					FLS
T2-1	Transverse deck	0.9	Direct welding through the deck hole	32	ULS
T2-2					
T2H-1					FLS
T2H-2					
T2H-3					
T2H-4					

(a) Temperature distributions

(b) Concrete slab during and after the heating process

Fig. 4 Thermal response of the specimens

K-type thermocouples were used to collect the temperatures of the web and flange. The gas temperature in the enclosure space between the specimen and electric furnace was measured at the middle height of the two levels of the shear stud.

3. Results and discussion

3.1 Temperature distribution

The push-out test specimens were heated according to the ISO 834 standard fire condition which shows a rapid temperature rise initially and a gradual increase afterwards. To illustrate the temperature boost region, the input current of the electric furnace was controlled to increase the enclosure temperature linearly up to 540℃ during the first 4 minutes. As indicated in Fig. 4(a), the gas temperature (T0) starts to increase linearly within a short period of time and complies with the ISO 834 fire curve after 4 minutes have elapsed.

The stud temperature at the shearing position is the critical parameter in determining the shear resistance as the failure mode is the stud shearing. Although the recommended stud temperature is 80% of the flange temperature in EC4-1-2 (CEN 2014b), this temperature ratio can be changed according to the experimental conditions, such as moisture content of the concrete slab, heating rate and shadow effect. Dara (2015) carried out a modified push-out test by placing a specimen into

a customised electric furnace. The temperature ratio between the shear stud and steel flange approached 90% to 95%. In the current study, the moisture in the concrete section smeared out to the back side of the slab during the heating process as shown in Fig. 4(b). In order to avoid the moisture disturbance during temperature measurement, a thermocouple was installed at the stud root through a hole that was created by drilling from the inside of the flange to the bottom of the stud shank. A temperature ratio of around 90% was obtained in the experiment.

The measured temperature data for different slab types were presented in Fig. 4(a). The web temperature shows a similar value throughout all types of specimens, while the flange temperature of the transverse deck specimen gives a higher value than the solid slab specimen. This temperature difference was caused by the additional area exposed to hot gas in the transverse deck as well as thermal conduction between the flange and concrete slab in the solid slab specimen. Zhao and Kruppa (1996) also found the temperature difference according to the slab types in composite beam experiments. The upper flange temperature of the rib deck specimen was higher than the solid slab specimen, while a similar temperature was observed at the web and bottom flange. It can be anticipated that the shear stud in the transverse deck slab is more vulnerable to fire than in the solid slab because the higher temperature of the stud root area was observed under the identical fire exposed condition.
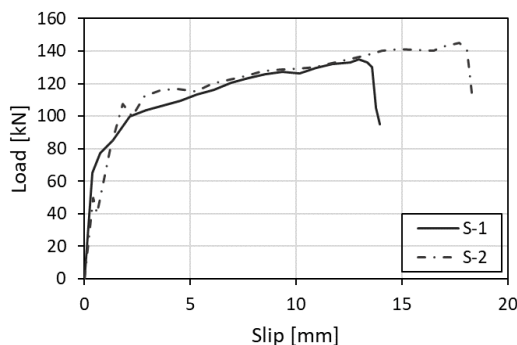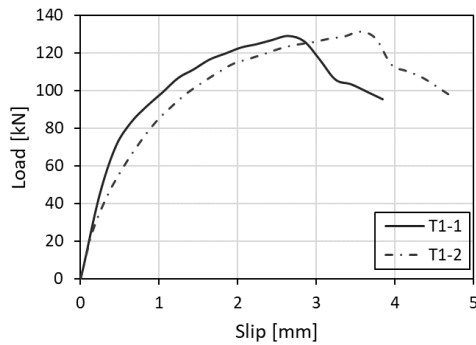

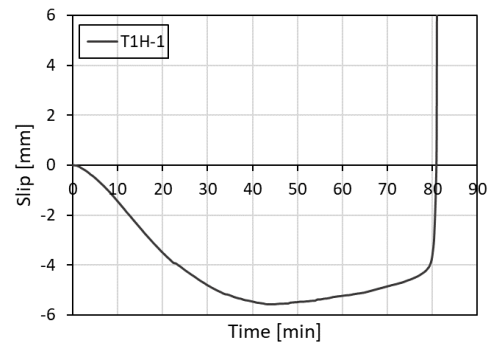(a) Load-slip relationship at room temperature
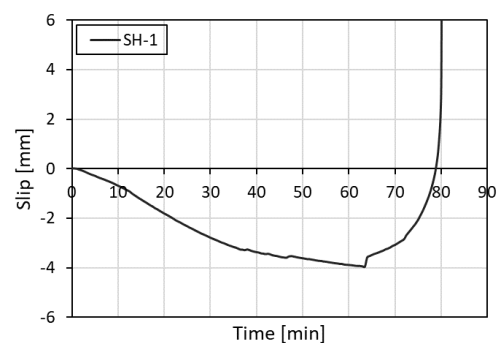
(b) Time-slip relationship at high temperature

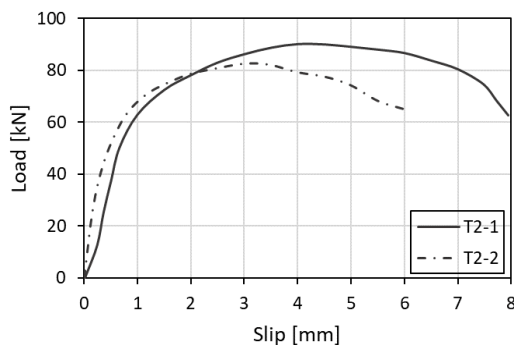Fig. 5 Structural response of the solid slab specimens

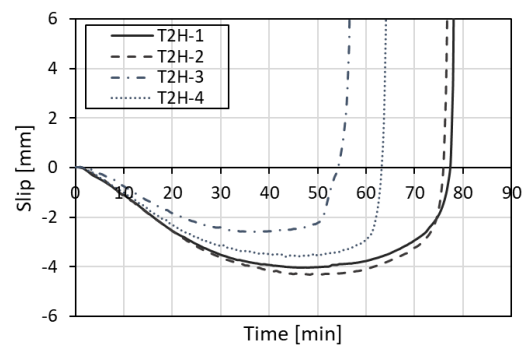(a) Load-slip relationship at room temperature

(b) Time-slip relationship at high temperature

Fig. 6 Structural response of the transverse deck specimens with through-deck welding

(a) Load-slip relationship at room temperature

(b) Time-slip relationship at high temperature

Fig. 7 Structural response of the transverse deck specimens with through-hole welding

3.2 Mechanical behaviour

The load-slip relationship at ULS and slip-time curve at FLS are plotted in Figs. 5-7 according to the specimen type. When the shear stud was embedded in a solid slab, the shear resistance consistently increased until the maximum load was reached in the ambient condition. Beyond the maximum resistance, the applied load decreased stepwise with a loud noise due to the stud tearing in the specimen. A different characteristic slip was observed depending on the fracture of each stud of four studs installed in a specimen. A constant load of 40.5 kN with the ISO 834 standard fire condition was applied to evaluate the shear resistance in a fire. The bottom of the shear stud was sheared after 80 minutes of the heating process. A negative slip was found at the beginning of the experiment owing to the thermal expansion of the steel and concrete sections, which indicates the thermal expansion force is higher than the applied load.

Two specimens were used to investigate the shear connection capacity in the 1.2 mm transverse deck slab at ULS, which gives an average resistance of 129 kN. Although the slip at the peak load was different, both experiments showed an analogous shear resistance as depicted in Fig. 6(a). This slip difference came from the heterogeneous property of concrete because the same failure mode of the concrete pull-out was found at both push-out tests. When 20.3 kN was applied continuously during the entire heating process, the stud shearing occurred

at the interlayer between the top flange and bottom of the stud weld collar after 81 minutes of heating. A negative slip was also observed during the heating process. It consistently increased for 40 minutes, and gradually decreased from 40 to 80 minutes of the heating process by virtue of thermal degradation of the shear connection, as plotted in Fig. 6(b). The slip value rapidly changes from the negative to positive direction at 81 minutes accompanied by the stud shearing failure.

When the shear stud was directly welded on the steel flange incorporating the 0.9-mm transverse deck with a 34-mm diameter hole, the average resistance of 86.5 kN was observed at ULS. The shear resistance reduces by 33% in comparison to the 1.2-mm deck specimen due to the deck thickness, stud welding method and concrete strength. In high-temperature experiments, the longer fire resistance time and higher negative slip were observed in the smaller initial load model, as shown in Fig. 7(b). The stud root area was sheared 77 minutes into the heating process when the initial loading of 30.4 kN was induced (T2H-3, T2H-4); both experiments show a comparable slip-time behaviour. Approximately 8 min of deviation was observed in the 45.6 kN models (T2H-1, T2H-2) because of the concrete crushing around the shear stud.

The obtained shear resistance was compared to the EC4-1-1 (CEN 2009) and ANSI 360-10 (2010), as presented in Table 2. The design guidance of EC4-1-1 (CEN 2009) gives a conservative estimate regardless of the slab type, while ANSI 360-10 (2010) predicts a higher load in the 0.9 mm

Table 2 Comparison of the shear resistance at ULS

Specimen	P_e [kN]	$P_{e,Rk}$ [kN]	P_{EC4} [kN]	P_{ANSI} [kN]	$P_{e,Rk}/P_{EC4}$	$P_{e,Rk}/P_{ANSI}$	Failure mode
S-1	135	121.5	107.5	100.8	1.13	1.2	Stud shearing
S-2	145						
T1-1	130	115.2	102	100.8	1.13	1.14	Concrete pull-out
T1-2	128						
T2-1	90	74.7	68	100.5	1.1	0.74	Concrete pull-out
T2-2	83						

(a) At room temperature (S-1)   (b) At high temperature (SH-1)
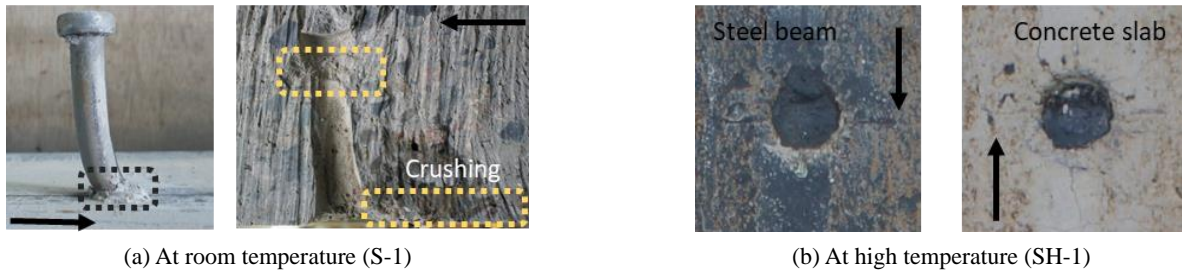
Fig. 8 Failure mode of the solid slab specimens
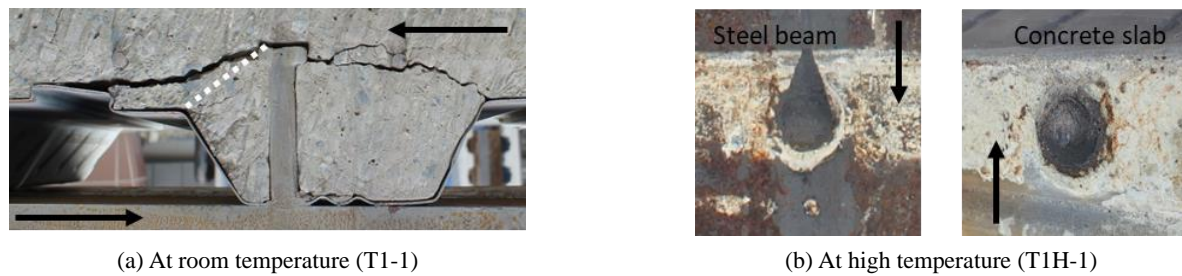
(a) At room temperature (T1-1)   (b) At high temperature (T1H-1)

Fig. 9 Failure mode of the trapezoidal deck specimens with through-deck welding

(a) At high temperature (T2H-3)   (b) At high temperature (T2H-1)

Fig. 10 Failure mode of the trapezoidal deck specimens with through-hole welding

deck specimen since it does not consider the deck thickness and welding method. The analytical calculation of EC4-1-1 (CEN 2009) provides a conservative estimate because a scattering factor is included in the characteristic shear resistance formula to consider the deviations among available experimental data based on the statistical study. Therefore, the deck thickness and stud welding method should be considered when calculating the shear resistance in the transverse deck applications at ULS.

3.3 Failure mode

The stud shearing failure was observed in the solid slab specimens under ambient and fire conditions with a different shearing location. The shearing occurred right above the weld collar, and the surrounding concrete was crushed in the loading direction at ULS. The overly bent stud shank is depicted in Fig. 8(a). In the high-temperature experiment, the boundary between the flange and the bottom of the weld collar was sheared off, as shown in Fig. 8(b). Higher thermal degradation of the flange shifted the shearing location down by virtue of the temperature gradient in composite beams.

Different failure modes were observed according to the temperature in the transverse deck specimens. The concrete pull-out failure was found at ULS, whereas the stud

shearing occurred at FLS. Considering heat paths and thermal conductivity of steel and concrete materials, the stud root area exhibits a higher temperature compared to the surrounding concrete. This higher thermal degradation of the steel material is the cause of the failure mode change. Concrete cracking around the shear stud was observed at ULS when examining the sliced specimen as provided in Fig. 9(a). This indicates that the shear resistance is determined not by the ultimate stud strength but by the concrete cracking caused by the rotation of the concrete rib. The crack started from the deck stiffener and extended to the deck shoulder through the stud head, which means the deck stiffener can be an influencing factor in determining the shear resistance in modern trapezoidal deck constructions. It makes the concrete cracking surface larger than a deck that does not have the stiffener. The deck stiffener and deck shoulder were deformed in the downward direction because of the concrete failure surface and moment at the stud root. A small amount of concrete crushing was found near the stud root in the loading direction. At high temperatures, the shearing occurred at the bottom of the weld collar in the upper-level stud and the steel flange was peeled off in the lower level stud (Fig. 9(b)) which withstands a higher load than another stud. The failure mechanism of the stud shearing was the same as the solid slab specimen.

When the shear stud was directly welded to the steel flange via a deck hole, concrete crushing and cracking were the causes of the failure at room temperature. The failure mode also changes to the stud shearing as temperature rises. When 55% of the shear resistance at ULS was induced, the stud shearing and concrete crushing were observed simultaneously. As shown in Fig. 10(a), half of the stud shank was sheared because the stud shearing was accompanied with concrete crushing; the other three shear studs in the same specimen were completely detached. When a smaller load was applied, all the shear studs in the specimen were sheared off as depicted in Fig. 10(b), which is the same failure mechanism as the other types of specimens. Therefore, it can be concluded that the primary cause of the failure at high temperatures is the thermal degradation of the steel materials (stud and flange), regardless of the slab type.

3.4 Design consideration

The design guidance of EC4-1-1 (CEN 2009) provides formulas for calculating the shear resistance of the headed shear connector at ULS based on experimental investigations. The characteristic shear resistance in a solid slab can be predicted depending on the cause of failure; a smaller value is adopted for design among the following equations

$$P_{k,stud} = 0.8 f_u A_s \qquad (1)$$

$$P_{k,concrete} = 0.29 \alpha d^2 \sqrt{f_{ck} E_{cm}} \qquad (2)$$

where, $P_{k,stud}$ is the characteristic shear resistance caused by the stud failure, $P_{k,concrete}$ is the characteristic shear resistance caused by a concrete-dominated failure, f_u is the

ultimate tensile strength of the stud material [MPa], A_s is the cross-sectional area of the stud shank [mm^2], α is the height parameter of the shear stud ($\alpha = 0.2(h_{sc}/d + 1)$ when $3 \leq h_{sc} \leq 4$ and $\alpha = 1$ when $h_{sc}/d > 1$, h_{sc} is the overall nominal height of the stud [mm], d is the stud shank diameter [mm], f_{ck} is the characteristic compressive cylinder strength [MPa] and E_{cm} is the secant elastic modulus of concrete [MPa].

When a trapezoidal deck is laid transverse to supporting beams, a further reduction is required according to the deck geometry and welding method. The shear resistance of a solid slab specimen is multiplied by the deck reduction factor which is given by

$$k_t = \frac{0.7}{\sqrt{n_r}} \frac{b_0}{h_p} \left(\frac{h_{sc}}{h_p} - 1 \right) \qquad (3)$$

where k_t is the transverse deck reduction factor, n_r is the number of studs in a rib ($n_r \leq 2$), b_0 is the average breadth of the deck [mm], h_p is the deck height [mm] and h_{sc} is the overall nominal height of a stud connector [mm].

The characteristic shear resistance in a fire can be calculated incorporating the thermal degradation rate of the steel and concrete materials in EC4-1-2 (2014). The smaller value is also selected for a design regardless of the failure mode change which has been described in section 3.3. The shear resistance of the solid slab P_k and transverse deck reduction factor k_t are multiplied by the thermal degradation rate of materials as follows

$$P_{fi,k,stud} = P_{k,stud} k_t 0.8 k_{u,\theta} \qquad (4)$$

$$P_{fi,k,concrete} = P_{k,concrete} k_t k_{c,\theta} \qquad (5)$$

where $P_{fi,k}$ is the characteristic shear resistance under elevated temperatures, 0.8 is the empirical constant, $k_{u,\theta}$ is the ultimate strength reduction factor of steel at elevated temperatures, $k_{c,\theta}$ is the strength reduction factor of concrete at elevated temperatures and the 80% and 40% of the flange temperature is used to obtain $k_{u,\theta}$ and $k_{c,\theta}$ parameters, respectively.

The failure mode in the transverse deck specimen changes from a concrete-dominated failure such as a concrete pull-out and rib shearing to the stud shearing as the temperature rises (Chen et al. 2015). This phenomenon was also observed when two studs were embedded in a rib with a staggered position (Yasuda et al. 2008). This infers that the shear resistance increases with regard to the number of studs in a trough at high temperatures. The aforementioned literature and experimental results were compared to EC4-1-2 (2014) with reference to the failure mode in Fig. 11; the empty dot indicates the concrete-dominated failure, and the filled dot represents the stud shearing failure. The Eurocode guidance gives a highly conservative estimate especially when the shear resistance at ULS is comparatively small. All the observed failure modes were the stud shearing when the stud temperature exceeded around 600℃. The stud shearing was caused by an excessive load at the stud root area that is higher than the stud tensile strength and smaller than the capacity of the surrounding concrete at a given

(a) Solid slab and 1.2 t through-deck welded specimen

(b) 0.9 t through-hole welded specimen

(c) 1.2 t through-deck welded specimen (Chen *et al*. 2015)

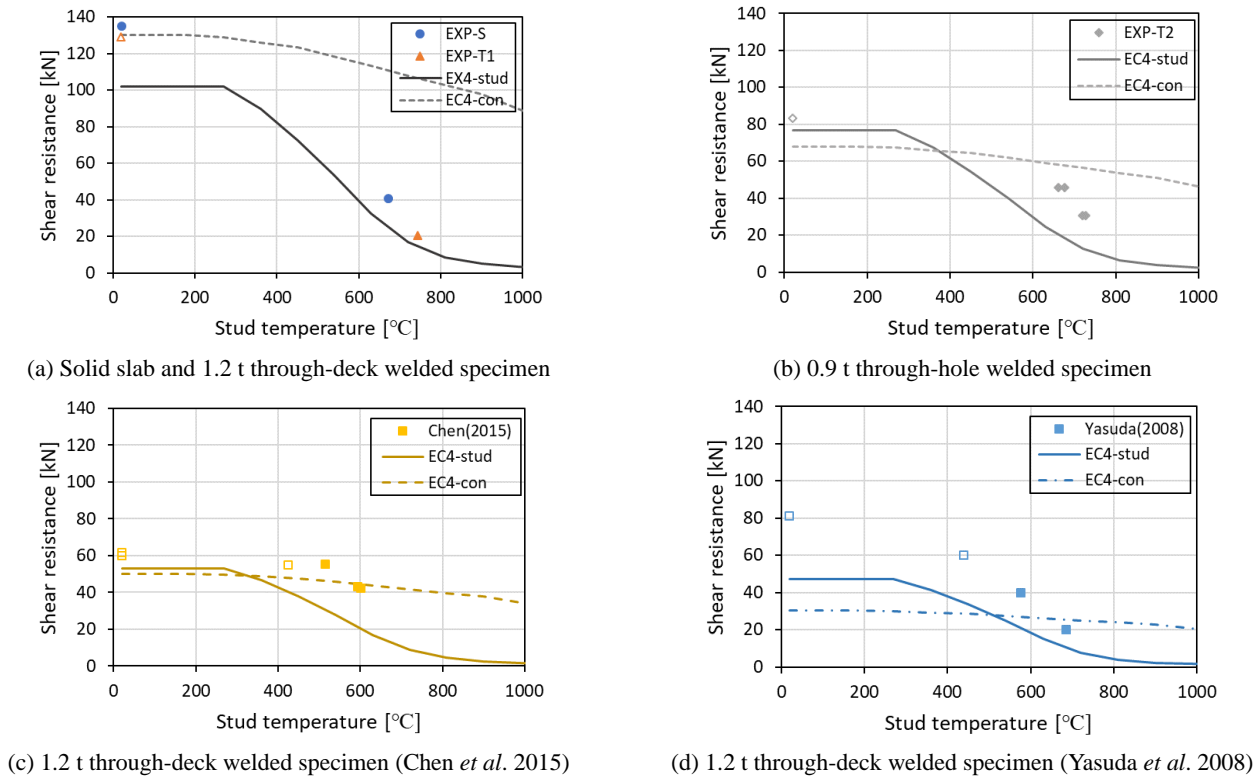(d) 1.2 t through-deck welded specimen (Yasuda *et al*. 2008)

Fig. 11 Comparisons of the experimental data and Eurocode guidance
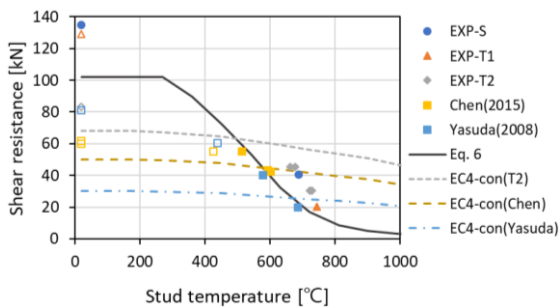

Fig. 12 Design considerations of shear resistance at FLS

temperature. It also proves that the most critical parameter at high temperature is the strength at the stud root area, which is the same cause of failure in the solid slab specimen.

When the high-temperature experimental data were compared to the analytical prediction of the stud shearing failure of EC4-1-2 (2014) without adopting the transverse deck reduction factor k_t, the Eurocode guidance successfully predicts the shear resistance regardless of the slab types as plotted in Fig. 12. Although the shear capacities at ULS were considerably different with respect to the deck geometry and stud welding method, the shear resistance under high temperatures converges on the solid slab design guidance when the failure mode was the stud shearing. Considering this experimental investigation, the shear resistance calculation method of the solid slab can be applied to the transverse deck application when the stud temperature exceeds around 600℃. Thus, a modified equation can be used to design the shear resistance at high

temperatures in the case of the stud shearing failure without regard to the slab type. Eq. (4) needs to be replaced by the following formula

$$P_{fi,k,stud} = P_{k,stud}0.8k_{u,\theta} \qquad (6)$$

where $P_{fi,k,stud}$ is the characteristic shear resistance caused by the stud failure under elevated temperatures.

The number of studs in a rib is a prominent influencing parameter in determining the shear resistance in a transverse deck slab at ULS, which has been argued regarding the relationship between the strength reduction ratio and the number of embedded studs. However, it also complies with the prediction of Eq. (6) when the stud shearing failure occurs. It can be deduced that the more a shear stud is embedded in a rib, the stronger the resistance of the shear connection at high temperatures.

4. Conclusions

The performance of the headed shear stud embedded in a transverse trapezoidal deck and solid slab at both ULS and FLS was investigated with regard to the slab type, deck thickness and stud welding method. Twelve push-out tests were conducted using a customised electric furnace to illustrate the ISO 834 standard fire condition, from which, the following conclusions were drawn:

- A deck stiffener affects the shape of the concrete cracking surface at ULS. A larger cracking area is expected when incorporating a modern trapezoidal deck.

- A relatively higher flange temperature is observed in the transverse deck specimen compare to the solid slab specimen, while an analogous temperature is measured at the web. Consequently, thermal degradation at the stud root area varies depending on the slab type under the same fire condition, which means utilising the solid slab is more robust to fire than adopting the transverse deck slab.

- A stud shearing failure is observed in all the solid slab specimens, whereas the failure mode changes from a concrete-dominated failure to the stud shearing in the transverse deck specimen as temperature rises. As the cause of failure is the stud shearing at FLS, the thermal degradation in the stud root area is a critical parameter in deciding the shear resistance regardless of the slab type. Thus, a new design formula is proposed by excluding the transverse deck reduction factor k_t based on the design guidance of EC4-1-2 (2014). It can be used in high temperature applications irrespective of the slab type.

- The capacity of the shear connection increases in accordance with the number of the studs embedded in a trough in the transverse deck slab when the expected failure mode is the stud shearing at elevated temperatures.

- Welding method and deck thickness are essential parameters to determine the shear resistance in transverse deck applications at ULS. However, its effect decreases as temperature rises because the cause of failure changes to the thermal degradation of the steel section.

References

ANSI/AISC 360-10 (2010), Specification for Structural Steel Buildings; American Institute of Steel Construction (AISC), Chicago, IL, USA.

CEN (2009), EN 1994-1-1:2004, Eurocode 4 - design of composite steel and concrete structures – Part 1-1: General rules and rules for buildings, European Committee for standardization, Brussel, Belgium.

CEN (2014a), EN 1992-1-1: 2004, Eurocode 2 - Design of concrete structures – Part 1-1: General rules for buildings, European Committee for standardization, Brussel, Belgium.

CEN (2014b), EN 1994-1-2, Eurocode 4 - design of composite steel and concrete structures – Part 1-2: General rules – Structural fire design, European Committee for standardization, Brussel, Belgium.

Chen, L.Z., Li, G.Q. and Jiang, S.C. (2012), "Experimental studies on the behavior of headed stud shear connectors at elevated temperatures", *Proceedings of the 7th International Conference on Structures in Fire*, Zurich, Switzerland, June.

Chen, L.-Z., Ranzi, G., Jiand, S.-C., Tahmaseninia, F. and Li, G.-Q. (2015), "Behaviour and design of shear connectors in composite slabs at elevated temperatures", *J. Constr. Steel Res.*, **115**, 387-397. https://doi.org/10.1016/j.jcsr.2015.08.025

Dara, S. (2015), "Behavior of the Shear Studs in Composite Beams at Elevated Temperatures", Ph.D. Dissertation; University of Texas at Austin, TX, USA.

Davoodnabi, S.M., Mirhosseini, S.M. and Shariati, M. (2019), "Behavior of steel-concrete composite beam using angle shear

connectors at fire condition", *Steel Compos. Struct., Int. J.*, **30**(2), 141-147. https://doi.org/10.12989/scs.2019.30.2.141

Ellobody, E. and Young, B. (2006), "Performance of shear connection in composite beams with profiled steel sheeting", *J. Constr. Steel Res.*, **62**(7), 682-694. https://doi.org/10.1016/j.jcsr.2005.11.004

He, Y.-L., Wu, X.-D., Xiang, Y.-Q., Wang, Y.-H., Liu, L.-S. and He, Z.-H. (2017), "Mechanical behavior of stud shear connectors embedded in HFRC", *Steel Compos. Struct., Int. J.*, **24**(2), 177-189. https://doi.org/10.12989/scs.2017.24.2.177

Hicks, S. (2009), "Strength and Ductility of Headed Stud Connectors Welded in Modern Profiled Steel Sheeting", *Struct. Eng. Int.*, **19**(4), 415-419. https://doi.org/10.2749/101686609789846975

ICC (2017), 2018 International Building Code (IBC), International Code Council, Inc., Washington DC, USA.

ISO (2016), ISO 6892-1, Metallic materials – Tensile testing – Part 1: Method of test at room temperature, International Organization for Standardization, Geneva, Switzerland.

Kumar, P. and Chaudhary, S. (2019), "Effect of reinforcement detailing on performance of composite connections with headed studs", *Eng. Struct.*, **179**, 476-492. https://doi.org/10.1016/j.engstruct.2018.05.069

Luo, Y., Hoki, K., Hayashi, K. and Nakashima, M. (2016), "Behavior and Strength of Headed Stud–SFRCC Shear Connection. I: Experimental Study", *J. Struct. Eng.*, **142**(2). https://doi.org/10.1061/(ASCE)ST.1943-541X.0001363

Mashiri, F.R., Mirza, O., Canuto, C. and Lam, D. (2017), "Post-fire Behaviour of Innovative Shear Connection for Steel-Concrete Composite Structures", *Structures*, **9**, 147-156. https://doi.org/10.1016/j.istruc.2016.12.001

McCam-Bartlett, S. (2019), Steel Construction Cost, Report of the British Constructional Steelwork Association and Steel for Life.

Nellinger, S., Odenbreit, C., Obiala, R. and Lawson, M. (2017), "Influence of transverse loading onto push-out tests with deep steel decking", *J. Constr. Steel Res.*, **128**, 335-353. https://doi.org/10.1016/j.jcsr.2016.08.021

Qi, J., Wang, J., Li, M. and Chen, L. (2017), "Shear capacity of stud shear connectors with initial damage: Experiment, FEM model and theoretical formulation", *Steel Compos. Struct., Int. J.*, **25**(1), 79-92. https://doi.org/10.12989/scs.2017.25.1.079

Qureshi, J., Lam, D. and Ye, J. (2011), "The influence of profiled sheeting thickness and shear connector's position on strength and ductility of headed shear connector", *Eng. Struct.*, **33**(5), 1643-1656. https://doi.org/10.1016/j.engstruct.2011.01.035

Rodrigues, J.P.C. and Laím, L. (2014), "Experimental investigation on the structural response of T, T-block and T-Perfobond shear connectors at elevated temperatures", *Eng. Struct.*, **75**, 299-314. https://doi.org/10.1016/j.engstruct.2014.06.016

Shahabi, S.E.M., Ramli Sulong, N.H., Shariati, M. and Shah, S. (2016), "Performance of shear connectors at elevated temperatures – A review", *Steel Compos. Struct., Int. J.*, **20**(1), 185-203. https://doi.org/10.12989/scs.2016.20.1.185

Sun, Q., Nie, X., Denavit, M.D., Fan, J. and Liu, W. (2019), "Monotonic and cyclic behavior of headed steel stud anchors welded through profiled steel deck", *J. Constr. Steel Res.*, **157**, 121-131. https://doi.org/10.1016/j.jcsr.2019.01.022

Wang, A.J. (2012), "Numerical investigation into headed shear connectors under fire", *J. Struct. Eng.*, **138**(1), 118-122. https://doi.org/10.1061/(ASCE)ST.1943-541X.0000428

Xu, C. and Sugiura, K. (2014), "Analytical investigation on failure development of group studs shear connector in push-out specimen under biaxial load action", *Eng. Fail. Anal.*, **37**, 75-85. https://doi.org/10.1016/j.engfailanal.2013.11.010

Yasuda, S., Michikoshi, S., Kobayashi, Y. and Narihara, H. (2008), "Experimental study on shear strength of headed stud shear

connectors at high temperature", *J. Struct. Constr. Eng.* (Trans. of AIJ), **73**(630), 1417-1423. https://doi.org/10.3130/aijs.73.1417

Zhao, B. and Kruppa, J. (1996), "Experimental and numerical investigation of fire behavior of steel and concrete composite beams", *Proceedings of Engineering Foundation Conference*, ASCE, New York, NY, USA, June.

CC